Supplement Information for "Reduction of Thermal Conductivity in Silicene Nanomesh: Insights from Coherent and Incoherent Phonon Transport"

Liu Cui [1, 2, †], Sanqiang Shi [2], Zhao Li [1], Gaosheng Wei [1], Xiaoze Du [1, †]

[1] *Key Laboratory of Condition Monitoring and Control for Power Plant Equipment, Ministry of Education, North China Electric Power University, Changping, Beijing 102206, China*

[2] *Department of Mechanical Engineering, The Hong Kong Polytechnic University, Hung Hom, Kowloon, Hong Kong, China*

[†] To whom correspondence should be addressed.

E-mail: liucui@ncepu.edu.cn (L. Cui); duxz@ncepu.edu.cn (X. Du)

1. Validation of the SW1 Potential Used

The nanoholes in SNMs are essentially a cluster of vacancy defects. The monovacancy, divacancy and Stone-Wales defect formation energies are often used to characterise the stability of the system with defects [1]. Rakib et al. [2] have computed the formation energy of silicene for monovacancy, divacancy and Stone-Wales defects using SW1 potential used in our study. They have found that the vacancy formation energies obtained by SW1 potential are in good agreement with the density functional theory (DFT) investigation. In addition, the error in the vacancy formation energies obtained by SW1 potential compared to DFT results is not increasing with the increase in the number of vacancies. This implies that the SW1 potential can describe reasonably well the structure and energetics of nanoholes in SNMs where the bond lengths and bond angles deviate from their equilibrium values. The SW1 force field has enough flexibility to describe a number of different configurations of silicene. It has been used, for example, to study the crack propagation behaviour in nanocrystalline silicene [2], the thermal conductivity of polycrystalline silicene with vacancy defects [3], and the thermal conductivity of silicene with isotope substitution [4].

2. Under-coordination Effect

The hybridization of Si atoms in the hole edges may be different from the Si atoms in other regions inside the system. As shown in Fig. S1, there are 6 under-coordinated atoms (displayed as red colour) whose coordination number is 2 near the nanohole. A previous study has reported that the bond between under-coordinated atoms

(displayed as yellow colour) becomes shorter and stronger [5]. Bond shortening and strengthening not only raises the local density of charge, mass and energy but also deepens the local potential, providing perturbation to the local potential [6]. This under-coordination effect raises the local energy density, or the elastic modulus, and subsequently the trap for electron transportation [6, 7].
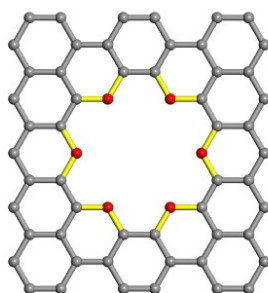

Figure S1. Schematic description of silicene nanomesh. The coordination number of silicon atoms in silicene is 3. There are 6 under-coordinated atoms displayed as red colour whose coordination number is 2 near the nanohole, and bonds displayed as yellow colour between the under-coordinated atoms near the nanohole become stronger.

The under-coordination effect also alters the phonon transportation. Xie et al. [6] have reported that, in addition to the missing mass and missing linkages, the change of force constant of bonds between the under-coordinated atoms near the nanoholes also results in phonon scattering. On the other hand, the localized edge modes (whose localization origins from the edge configuration and core is the edge atoms) may appear [8, 9]. The vibrational amplitude of the localized edge modes decreases to zero very quickly from edges into center [10, 11].

3. Phonon lifetime

In this paper, the phonon lifetimes were estimated from the spectral energy density

(SED) [12-14]. The following formula is used to calculate the phonon SED function Φ [12]

$$\Phi\left(\boldsymbol{\kappa},\omega\right)=\frac{1}{4\pi\tau_0 N_{\mathrm{T}}}\sum_{\alpha}^{}\sum_{b}^{B}m_b\left|\int_0^{\tau_0}\sum_{n_{x,y,z}}^{N_{\mathrm{T}}}\dot{u}_\alpha\left(\begin{matrix}n_{x,y,z}\\b\end{matrix};t\right)\times\exp\left[i\boldsymbol{\kappa}\cdot\mathbf{r}\left(\begin{matrix}n_{x,y,z}\\0\end{matrix}\right)-i\omega t\right]\mathrm{d}t\right|^2 \tag{1}$$

where $\boldsymbol{\kappa}$ is the wave vector, ω is the angular frequency, τ_0 is the total integration time, and α represents the x, y or z direction. There are N_{T} unit cells in the system, and each unit cell contains B atoms. m_b is the mass of b-th atom. $\dot{u}\left(\begin{matrix}n_{x,y,z}\\b\end{matrix},t\right)$ is the velocity of b-th atom in the $n_{x,y,z}$-th SED unit cell at time t. $r\left(\begin{matrix}n_{x,y,z}\\0\end{matrix}\right)$ is the equilibrium position of each unit cell. In this work, $\boldsymbol{\kappa}$ is in the heat flux direction, which is corresponding to zigzag direction of silicene in real space. We used a diatomic silicene unit cell described in Ref. [13], and chose a fixed simulation domain of $N_x = N_y = 20$ for the in-plane direction. After structure relaxation with Nosé-Hoover thermostats, the system was run under the NVE ensemble for 2 ns, and the atomic velocities were collected every 5 fs.

Alternatively, if the atomic velocities are represented by the normal mode coordinates, the SED function (Eq. (1)) can be written as the sum of Lorentzian functions of all phonon branches [13, 15, 16]

$$\Phi\left(\boldsymbol{\kappa},\nu\right)=\sum_{\nu}^{3B}\frac{I\left(\boldsymbol{\kappa},\nu\right)}{1+\left\{\left[\omega\left(\boldsymbol{\kappa},\nu\right)-\omega_C\left(\boldsymbol{\kappa},\nu\right)\right]/\gamma\left(\boldsymbol{\kappa},\nu\right)\right\}^2} \tag{2}$$

where ν is the phonon branch index, $I(\boldsymbol{\kappa}, \nu)$ is the peak magnitude, $\omega_C(\boldsymbol{\kappa}, \nu)$ is the frequency at the peak center, and $\gamma(\boldsymbol{\kappa}, \nu)$ is the half-width at half-maximum. There exist $3B$ peaks (including the degenerate peaks) at each $\boldsymbol{\kappa}$ point. The lifetime of phonon mode $(\boldsymbol{\kappa}, \nu)$ can be calculated as

$$\tau\left(\mathbf{\kappa},\nu\right)=\frac{1}{2\gamma\left(\mathbf{\kappa},\nu\right)} \qquad (3)$$

References

1.   J. Gao, J. Zhang, H. Liu, Q. Zhang and J. Zhao, *Nanoscale*, 2013, 5, 9785-9792.
2.   T. Rakib, S. Saha, M. Motalab, S. Mojumder and M. M. Islam, *Scientific Reports*, 2017, 7, 14629.
3.   Y. Gao, Y. Zhou, X. Zhang and M. Hu, *The Journal of Physical Chemistry C*, 2018, 122, 9220-9228.
4.   S. Srinivasan, U. Ray and G. Balasubramanian, *Chemical Physics Letters*, 2016, 650, 88-93.
5.   C. Q. Sun, *Progress in Solid State Chemistry*, 2007, 35, 1-159.
6.   G. Xie, Y. Shen, X. Wei, L. Yang, H. Xiao, J. Zhong and G. Zhang, *Scientific Reports*, 2014, 4.
7.   T. A. Yeung, T. Chiam, C. Chen, C. Sun, W. Shangguan, W. Wong and C. Kam, *Physical Review B*, 2005, 72, 155417.
8.   J. Jiang, J. Chen, J. Wang and B. Li, *Physical Review B*, 2009, 80, 052301.
9.   J. Jiang and J. Wang, *Physical Review B*, 2010, 81, 174117.
10.   R. Bell and P. Dean, *Discussions of the Faraday Society*, 1970, 50, 55-61.
11.   A. Bodapati, P. K. Schelling, S. R. Phillpot and P. Keblinski, *Physical Review B*, 2006, 74, 245207.
12.   J. A. Thomas, J. E. Turney, R. M. Iutzi, C. H. Amon and A. J. McGaughey, *Physical Review B*, 2010, 81, 081411.
13.   Z. Wang, T. Feng and X. Ruan, *Journal of Applied Physics*, 2015, 117, 084317.
14.   T. Feng, X. Ruan, Z. Ye and B. Cao, *Physical Review B*, 2015, 91, 224301.
15.   B. Qiu and X. Ruan, *Applied Physics Letters*, 2012, 100, 193101.
16.   C. Li, G. Li and H. Zhao, *Journal of Applied Physics*, 2015, 118, 075102.